(8) C. E. Blackburn, *J. Labelled Compd.*, 8, 279 (1972).
(9) (a) V. C. Jordan, C. J. Dix, K. E. Naylor, G. Prestwich, and L. Rowsby, *J. Toxicol. Environ. Health*, 4, 363 (1978); (b) F. Capony and H. Rochefort, *Mol. Cell. Endocrinol.*, **11**, 181 (1978).
(10) D. Lednicer, D. E. Emmert, G. W. Duncan, and S. C. Lyster, *J. Med. Chem.*, **10**, 1051 (1967).
(11) D. Lednicer, D. E. Emmert, S. C. Lyster, and G. W. Duncan, *J. Med. Chem.*, **12**, 881 (1969).
(12) This hexahydrodiol product was only characterized by mass spectrometry; it is assigned the structure **4b** by analogy with the phenol **4a**, whose structure was further ascertained by other spectroscopic means (See Experimental Section).
(13) Careful ^{1}H NMR analysis of the starting phenol **1a** and the alkylation product **1b** indicate that these materials contain a small amount (estimated to be 5–8%) of naphthalenic impurities. These materials are not effectively removed by recrystallization and preparative scale chromatography on silica gel. They are presumed to be the result of aromatization of the sensitive dihydronaphthalene system during the cyclization of the precursor **5**. Because of the presence of this naphthalenic material in **1a**, it is difficult to determine whether the compounds **3a** and **3b**, noted after the hydrogenation step, are the result of dehydrogenation or simply result from carry over of the naphthalenic impurities in our sample of **1a**.
(14) D. Lednicer, personal communication. B. S. Katzenellenbogen, unpublished.
(15) J. A. Katzenellenbogen, H. J. Johnson, Jr., and H. N. Myers, *Biochemistry*, **12**, 4085 (1973); J. A. Katzenellenbogen, K. E. Carlson, H. J. Johnson, Jr., and H. N. Myers, *ibid.*, **16**, 1970 (1977).
(16) J. A. Katzenellenbogen, D. F. Heiman, R. Goswami, K. J. Allison, and K. E. Carlson, in preparation.
(17) J. M. Fromson, S. Pearson, and S. Bramah, *Xenobiotica*, **3**, 693 and 711 (1973).
(18) A. F. Rosenthal and R. P. Geyer, *J. Am. Chem. Soc.*, **80**, 5240 (1958).
(19) J. B. Schenkman, H. Remmer, and R. W. Estabrook, *Mol. Pharmacol.*, **3**, 113 (1967).
(20) K. J. Netter and G. Geidel, *J. Pharmacol. Exp. Ther.*, **146**, 61 (1964).

Electrostatic Potentials of Deoxydinucleoside Monophosphates. 1. Deoxydinucleoside Monophosphates and Actinomycin Chromophore Interactions

Merrill E. Nuss and Peter A. Kollman*

Department of Pharmaceutical Chemistry, School of Pharmacy, University of California, San Francisco, California 94143.
Received June 7, 1979

We present electrostatic potential maps for the ten Watson–Crick base-pair combinations of dinucleoside monophosphates in a conformation appropriate for intercalation of drugs to occur. These maps reveal interesting differences among the base-pair combinations and suggest reasons for the base-pair specificities often observed upon intercalation. Simple electrostatic calculations on the intercalation energy of substituted actinomycin chromophores correlate qualitatively with the relative biological activity of these compounds, although the correlation with binding affinity is not as satisfactory.

The importance of drug–DNA interactions has long been recognized. An important step in our molecular level understanding of such processes was made with Lerman's suggestion[1] that flat, planar drugs could "intercalate" between the bases of the DNA. Because the base–base distance along the helical axis in normal double-stranded DNA is only 3.4 Å, there must be a considerable conformational change in the DNA backbone (sugar and phosphate) for a drug to be able to intercalate. The resulting conformation of the backbone must have a base–intercalator separation of ~3.4 Å and thus a base–base separation of ~6.8 Å. Specific stereochemical models for DNA intercalation have been developed by Sobell[2] and Alden and Arnott.[3] The former is based on a high-resolution X-ray structure of the deoxyguanosine–actinomycin D complex and the latter on general stereochemical considerations. Although they differ somewhat in the values proposed for the backbone structure, both studies conclude that the DNA base–base distance can be increased to ~6.8 Å without appreciable "strain".[4]

Another very interesting realization has been the base specificity of different intercalators. Sobell,[2] Krugh,[5] and Müller and Crothers[6] have documented specific examples of base specificity; in particular, Sobell and Krugh have noted that actinomycin D (1) prefers to intercalate between G-C H-bonded base pairs.

We have been interested in the electrostatic potentials surrounding globular proteins in the hope of developing

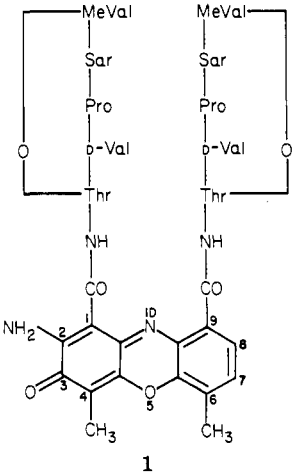

1

simple models for protein–substrate interactions.[7] Interesting applications of the electrostatic potential have been made in the analysis of the structure–activity relationships of hallucinogens,[8] cholinergics,[9] and narcotic analgetics.[10] Theoretical and experimental studies on small polar molecule gas-phase interactions are consistent with the view that the electrostatic component of the interaction energy is the dominant one.[11] We thus chose to develop a simple electrostatic model for DNA–intercalator interactions. Our interest was particularly stimulated by these interactions,

0022-2623/79/1822-1517$01.00/0

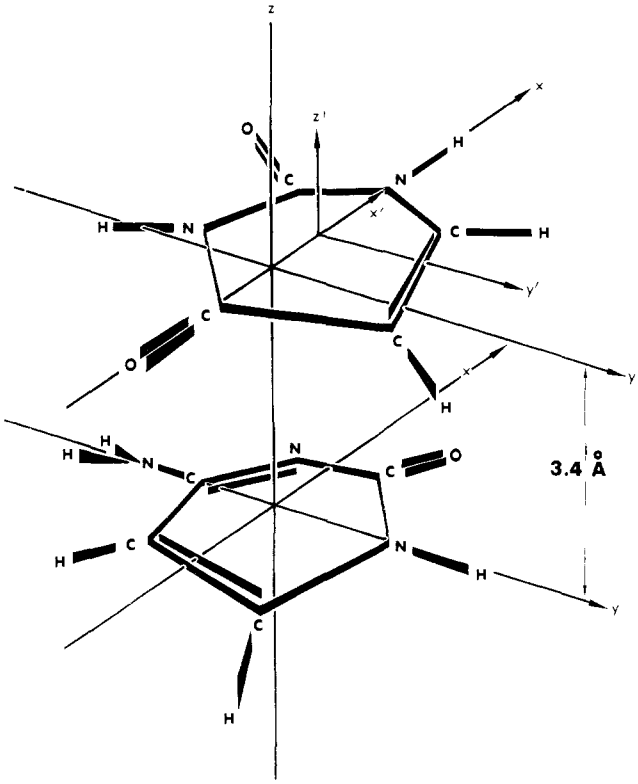

Figure 1. The relative position of uracil and cytosine. Uracil has been displaced along the x axis with $y = 0$ and $\theta = 0$.

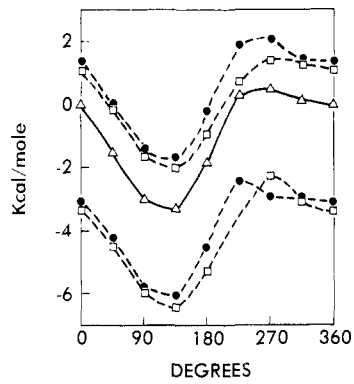

Figure 2. The interaction energy (kcal) of cytosine and uracil (see Figure 1) as a function of θ, the angle of clockwise rotation of uracil relative to its position in Figure 1. The solid circles represent the interaction energy using CNDO/2 partial charges for the bases, while the open squares use ab initio charges. The circles and squares on top represent the interaction between the two bases without Lennard–Jones $(L–J)^{12}$ terms, while the ones on the bottom have included the L–J dispersion attraction and exchange repulsion contributions. The interaction energy was also calculated using the CNDO/2 method (triangles).

since they probably are the "drug–receptor" complex best characterized at the molecular level as well as one of those most amenable to detailed theoretical study.

In this paper, we attempt to show (1) that intercalator–base specificity is influenced by the different electrostatic potentials of the ten base-pair combinations and (2) that substituents on actinomycin can have a substantial effect on the electrostatic intercalation energies.

Results and Discussion

We first studied the interaction of uracil and cytosine with the center of the molecules 3.4 Å apart and the planes of the molecules parallel (Figure 1). We then rotated the uracil with respect to the cytosine and evaluated the energy

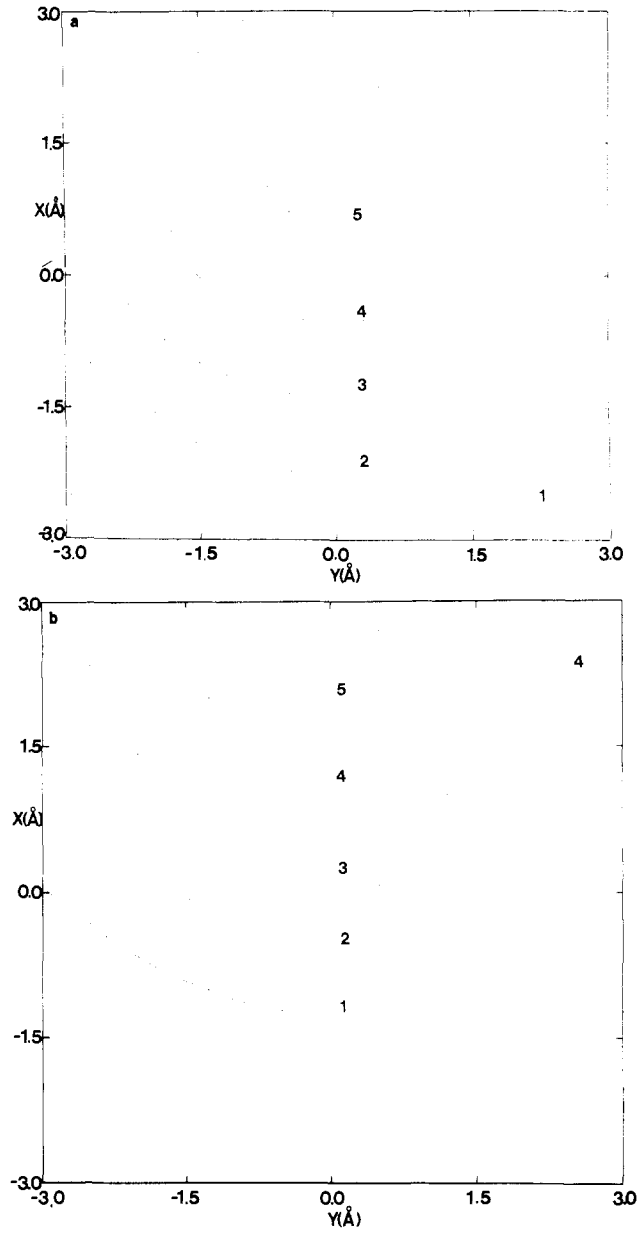

Figure 3. (a) This drawing plots the interaction energy of cytosine and uracil (see Figure 1) using electrostatic, dispersion attraction, and exchange repulsion terms as a function of X, Y, and θ. At each X and Y value, the minimum energy value for θ is represented on the diagram. The following numbers are used to represent the interaction energy contours (kcal): 1 = –2.5; 2 = –3.5; 3 = –4.5; 4 = –5.5; 5 = –6.5. (b) Only the electrostatic contribution to the interaction energy is plotted here. The following numbers are used to represent the interaction energy contours (kcal): 1 = –0.6; 2 = –1.2; 3 = –1.8; 4 = –2.4; 5 = –2.8.

with the CNDO/2 method, with the partial charges derived from CNDO/2 and STO-3G ab initio, and with the ab initio partial charges plus a reasonable set of Lennard–Jones potential terms.[16] The results of these calculations are presented in Figure 2 and demonstrate that (1) the relative energies are dominated by the electrostatic term and (2) the CNDO/2 electrostatic charges do a good job in mimicking the minimal basis ab initio charges. Dispersion attraction does not change the directionality of the interaction. In all four calculations, the minimum energy occurred at $\theta \sim 125°$.

The magnitude of the dispersion attraction for these planar "stacking" interactions is substantial, however. If one relaxes the constraint of forcing the center of the two molecules to be on top of each other, we now have three

Table I. STO-3G Derived Partial Charges for Nucleotides

sugar-phosphate backbone		adenine		guanine		thymine		cytosine	
atom	partial charge[a]	atom	partial charge[a]	atom	partial charge[a]	atom	partial charge[a]	atom	partial charge[a]
C1	0.180			N1	−0.361	N1	−0.226	N1	−0.217
H1	0.056	N1	−0.319	H1	0.218	C2	0.421	C2	0.366
C2	−0.132	C2	0.147	C2	0.388	O2	−0.305	O2	−0.314
H2A	0.085	H2	0.082	N2	−0.420	N3	−0.380	N3	−0.357
H2B	0.059	N3	−0.298	H2A	0.240	H3	0.231	C4	0.272
C3	0.008	C4	0.199	H2B	0.218	C4	0.294	N4	−0.415
H3	0.028	C5	0.004	N3	−0.353	O4	−0.279	H4A	0.233
C4	0.060	C6	0.262	C4	0.201	C5	−0.049	H4B	0.213
H4	0.072	N6	−0.414	C5	−0.022	C6	0.071	C5	−0.138
O1	−0.265	HA6	0.227	C6	0.299	H6	0.091	H5	0.065
C5	0.007	HB6	0.226	O6	−0.284	C7	−0.176	C6	0.100
H5A	0.054	N7	−0.281	N7	−0.252	H7A	0.079	H6	0.094
H5B	0.068	C8	0.152	C8	0.126	H7B	0.062		
O3	−0.477	H8	0.093	H8	0.084	H7C	0.068		
P	1.343	N9	−0.178	N9	−0.180				
OA	−0.738								
OB	−0.738								
O5	−0.477								
Na^+	1.0								

[a] Partial charges employed in electrostatic potential calculations in atomic units. The above charges were used for dinucleoside phosphates with the sugar above on the 5' end. The 5' sugar also had charges O5 (−0.338) and HO5 (0.194). For the 3' end sugar, the following charges were used: O3 (−0.309), HO3 (0.197), C5 (−0.033), H5A, H5B (0.032) and the remaining charges as in the 5' sugar.

degrees of freedom to vary: the position of the center of the uracil molecule (two variables, X and Y) and the angle it makes with the Z axis (one variable, θ). The minimum energy in such a surface (ab initio electrostatic charges plus Lennard–Jones) is at $X = 1.5$, $Y = 0.0$, $\theta = 90.0$ and is illustrated in Figure 3a. Both the electrostatic energy and dispersion attraction are substantially attractive at this point. The minimum energy predicted from varying the electrostatic energy alone is at $X = 2.0$, $Y = 0.0$, and $\theta = 90.0$ (see Figure 3b). Again, it appears that, although dispersion attraction is very important, the relative electrostatic term dominates the *directionality* of the interaction.

Next we examine the electrostatic potential in the plane of the actinomycin chromophore (1) due to the presence of the dinucleotide base pair. As noted above, we used the Sobell geometry for the chromophore plane and the dinucleotide base pair and the sodium salt of the anion. We examined the electrostatic potential for all ten base-pair combinations and these are illustrated in Figures 4a–j. The projection of G-C base pairs and A-T base pairs onto this plane are illustrated in Figure 5; the location of the actinomycin chromophore is illustrated in Figure 6.

The differences in electrostatic potential for different base-pair combinations are quite noticeable and of potential utility as an aid in understanding base specificity for different intercalators. For most of the base-pair combinations, the most negative potential is in the top part of the figure and thus one would expect electropositive groups to prefer to be in this region. These electrostatic potential maps show (1) that one should expect significant base specificity in intercalator interactions and (2) that one can use substituent effects in intercalators to design molecules with increased base-pair specificity and stronger binding. For example, electronegative substituents at the 6 position might (generally) be expected to increase binding and those at the 8 position to decrease binding (relative to the unsubstituted molecule).

We also analyzed the electrostatic potential for the anion (without Na^+) for $<^{GC}_{CG}>$ and $<^{CG}_{GC}>$. The contours are much larger in magnitude, so differences are harder to spot on the maps and we do not present them here. However, an examination of the individual grid points as well as a careful comparison of the maps shows that $<^{CG}_{GC}>$ has a more negative region in the center of the map than $<^{GC}_{CG}>$. The absence of the Na^+ counterions causes the phosphate negative potential to dominate the fine structure of the maps and makes them more difficult to interpret than Figure 4.

As a more precise test of this electrostatic model for analyzing substituent effects, we studied the interactions of 2- and 7-substituted actinomycin chromophores with the ten base-pair combinations. We kept the actinomycin chromophore (1) at the X-ray geometry and added substituents at standard geometries. We used the CNDO/2 Mulliken populations for the substituted actinomycins, including the phenoxazone rings and the two amide groups attached at the 1 and 9 positions. The N–C (Thr) linkages were replaced by N–H.

The electrostatic interaction energies between a chromophore and a dinucleotide base pair was evaluated and Table II contains the results. The significant base and substituent dependence of the interaction energies is quite clear. It is interesting that the actinomycin chromophore has the largest interaction energy with the $<^{CG}_{GC}>$ dinucleotide, in qualitative agreement with the experimental results. Table III contains the comparison between calculated interaction energies and experimental binding affinities of some of the substituted chromophores.

There is rather poor agreement between the calculated affinities and experimental affinities. However, if one focuses on the data in BPES buffer, the calculations are successful in reproducing the fact that the only compound with a significantly lower association constant than the others (the C–Cl compound) also has the smallest calculated interaction energy.

Interestingly, the agreement between the interaction energy and the in vivo activities (Table IV) is better than

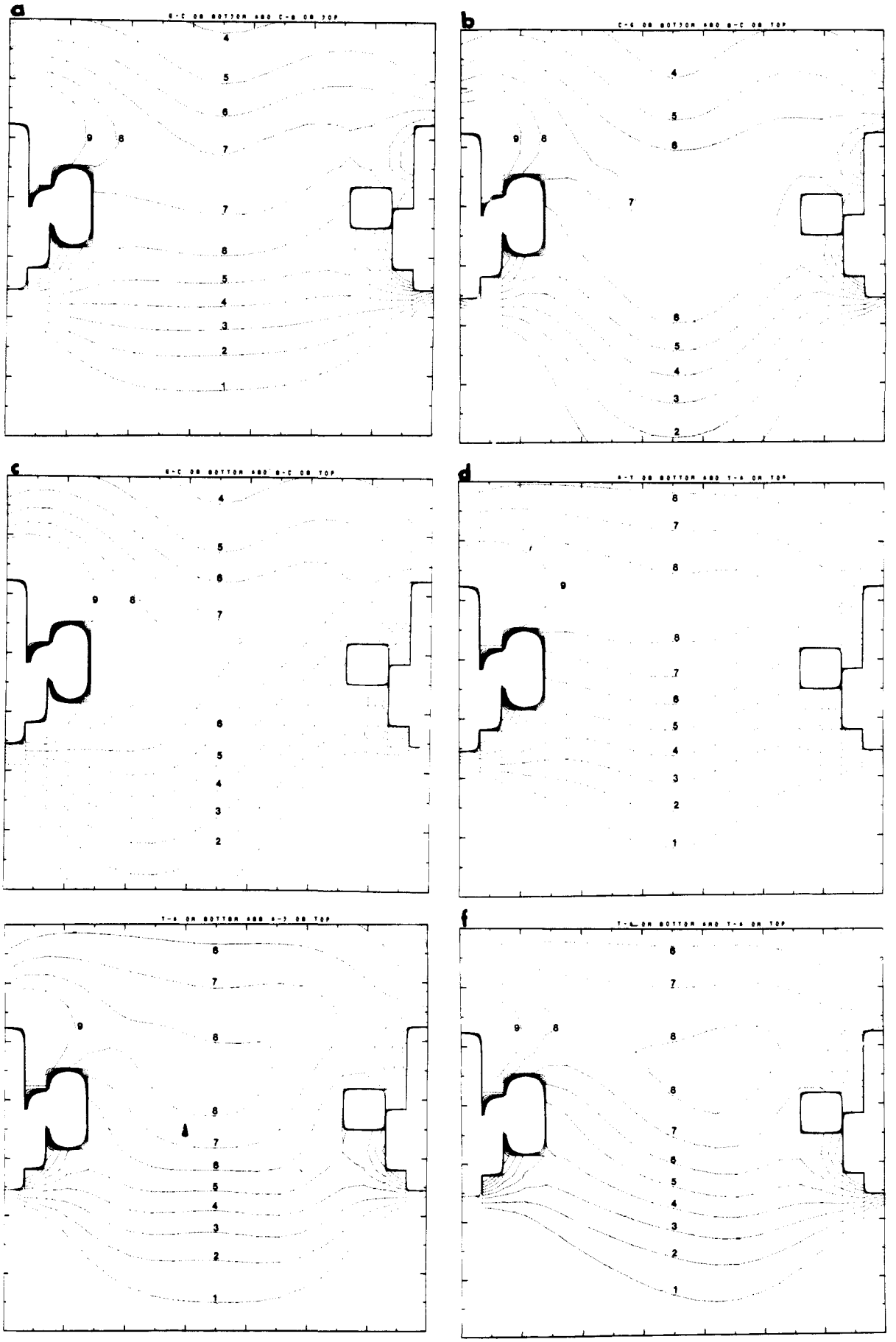
a
b
c
d
f

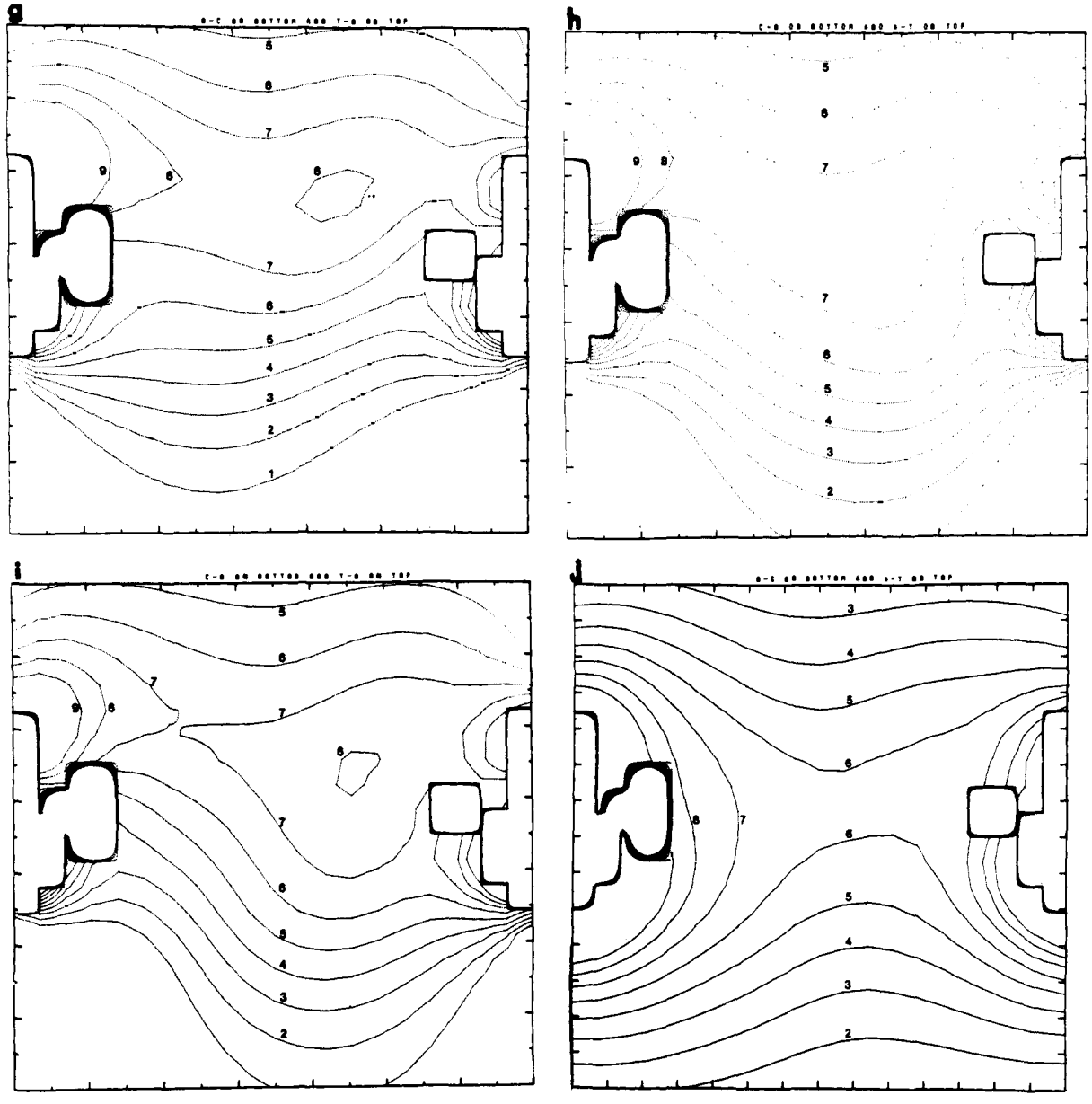

Figure 4. (a–j) Electrostatic potential contour maps in the plane of the actinomycin C chromophore for the ten different base-pair combinations of DNA including sodium atoms. The excluded volume on the side of the contour plots is due to the sugar–phosphate atoms of the nucleic acid backbone. Units for the electrostatic potential contours (q/r) are (atomic units/angstroms) × 100. The top of the contour plot denotes the minor groove of BDNA. The designation $\frac{G}{C}$ refers to guanine (3′-5′)cytosine as viewed from the major groove. The plot represents a surface (plane of actinomycin chromophore) that is 7 × 7 Å.

that between the interaction energy and the association constant. The four active compounds have a calculated interaction energy of −4.28 (standard deviation 0.17); the four inactive compounds have a calculated interaction energy of −3.38 (standard deviation 0.31).

As we have pointed out before, the Sobell and Alden and Arnott models differ in the intercalation structural parameters for the sugar–phosphate backbone, but these differences may not effect our calculated *base specificities*.

The Mulliken populations are relatively geometry independent, and we used standard geometries to derive the populations. We have also further broken down the intercalation energies into atom–atom contributions. The two amide groups on the actinomycin chromophore do play an important role in the base specificity, as has been suggested by Sobell.[2] Table IV compares the interaction energies for the different base pairs with and without the amide side chains.

It should be emphasized here that out interaction energy calculations are very crude; they leave out many important

Scheme I

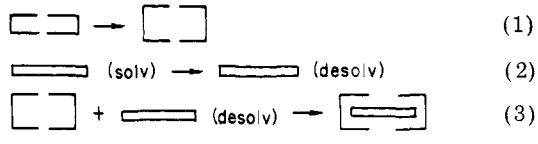

facts. We envisage the intercalation process to proceed as shown in Scheme I, where step 1 involves conformational change and unstacking energies of the base pairs, step 2 the desolvation of the intercalator, and step 3 the interaction of 6.8 Å separated base pairs and intercalator.

We have focused our attention mainly on the energy of step 3 and are currently carrying out analyses of steps 1 and 2 by classical conformational analysis [(1)] and simple empirical solvation energy estimates [(2)]. However, we should point out that the use of only step 3 in the comparison of the relative interaction energies for *isomers*, e.g., 2-H, 7-NH_2 compared to 2-NH_2, 7-H should be close to correct.

Table II. Interaction Energies for Actinomycin Chromophore with Dinucleoside Monophosphates[a]

substitn		dinucleoside monophosphate[b]									
2	7	G-C / G-C	G-C / C-G	C-G / G-C	T-A / T-A	T-A / A-T	A-T / T-A	T-A / C-G	A-T / C-G	A-T / G-C	T-A / G-C
H	H	−1.87	−3.35	−3.29	−2.22	−1.52	−1.35	−3.43	−2.56	−1.08	−1.95
OH	H	−2.15	−3.18	−3.25	−1.84	−1.33	−1.17	−2.97	−2.30	−1.27	−1.94
NH_2	H	−3.30	−4.06	−4.41	−2.76	−2.51	−2.06	−3.89	−3.19	−2.42	−3.12
NO_2	H	+2.31	−0.79	+0.54	+0.10	+1.91	+1.05	−1.24	−0.29	+2.80	+1.85
F	H	−0.73	−2.48	−1.96	−1.23	−0.15	−0.51	−2.32	−1.60	+0.15	−0.57
Cl	H	−1.18	−2.70	−2.41	−1.39	−0.61	−1.39	−2.57	−1.83	−0.32	−1.06
Br	H	−1.47	−2.90	−2.72	−1.58	−0.89	−0.82	−2.79	−2.03	−0.60	−1.36
H	OH	−1.02	−2.78	−2.36	−1.48	−0.58	−0.91	−2.76	−2.19	−0.43	−1.01
H	NH_2	−0.98	−3.15	−3.60	−2.71	−1.61	−1.17	−4.12	−2.57	−0.41	−1.95
H	NO_2	−3.33	−3.97	−2.48	−1.87	−1.54	−2.04	−2.70	−2.87	−2.22	−2.06
H	F	−2.47	−3.74	−2.83	−2.05	−1.40	−1.73	−3.16	−2.83	−1.56	−1.89
H	Cl	−2.40	−3.69	−2.54	−1.82	−1.15	−1.62	−2.93	−2.74	−1.45	−1.65
H	Br	−2.00	−3.55	−3.23	−2.51	−1.74	−1.72	−3.64	−2.85	−1.29	−2.10
NH_2	OH	−2.31	−3.28	−3.26	−1.61	−1.19	−1.25	−2.85	−2.49	−1.53	−1.89
NH_2	NH_2	−2.22	−3.60	−4.40	−2.75	−2.11	−1.45	−4.11	−2.81	−1.43	−2.73
NH_2	NO_2	−4.78	−4.42	−3.41	−1.63	−1.94	−2.08	−2.51	−2.96	−3.32	−2.51
NH_2	F	−3.89	−4.46	−3.93	−2.60	−2.39	−2.44	−3.62	−3.47	−2.90	−3.62
NH_2	Cl	−3.37	−3.98	−3.86	−2.14	−1.93	−1.77	−3.29	−2.92	−2.31	−3.29
NH_2	Br	−3.23	−3.91	−3.94	−2.18	−1.94	−1.69	−3.36	−2.87	−2.19	−3.36

[a] Units are kcal/mol. [b] $\begin{matrix}\text{G-C}\\ \langle\ \rangle \\ \text{G-C}\end{matrix}$ has the left-hand chain 3′ on top; right-hand chain 5′ on top.

Table III. Comparison between Calculated Interaction Energies and DNA Binding Affinities of Actinomycin Analogues

compd[b]	DNA binding[a] buffer	$K_{ap} \times 10^{-6}$	interaction energy (max)[c]
Act. C3	BPES	2.4	−4.41
7-NO_2-Act. C3	BPES	3.05	−4.78
7-NH_2-Act. C3	BPES	3.2	−4.40
7-Br-Act. C3	BPES	7.0	−3.94
Act. C3	0.01 PO_4	12.0	−4.41
7-NO_2-Act. C3	0.01 PO_4	38.0	−4.78
7-NH_2-Act. C3	0.01 PO_4	38.0	−4.40
Act. C1	BPES	2.3	−4.41
7-OH-Act. C1	BPES	4.2	−3.28
2-Cl-Act. C1	BPES	0.025	−2.70

[a] See ref 6 for experimental results. [b] Actinomycin (abbreviated Act.) C1 = D differs from actinomycin C3 only in changes in the pentapeptide backbone. As one can see, this change has little effect on K_{ap} in BPES buffer.

Table IV. Comparison between Calculated Interaction Energies and in Vivo Bacteriostatic Activity

substituent[c]	activity	interaction energy (max)[c]
2-NH_2, 7-H (Act.)	+	−4.41
2-OH, 7-H	−	−3.25
2-Cl, 7-H	−	−2.70
2-NH_2, 7-NH_2	−	−4.40
2-NH_2, 7-OH	−	−3.28
2-NH_2, 7-Cl	+	−3.98
2-NH_2, 7-Br	+	−3.94
2-NH_2, 7-NO_2	+	−4.78

[a] See ref 17. [b] Maximum interaction energy of the ten base-pair combinations. [c] Act. = actinomycin.

The ΔS of intercalation is another important consideration and appears to be the dominant[19] thermodynamic variable for actinomycin D–DNA interactions (the interaction of charged intercalators with DNA appears, on the other hand, to be enthalpy dominated). In fact, without the peptide, intercalation for AcD is undetectable.[6] Our results (Table V) are consistent with very little *net* energetic attraction between the actinomycin chromophore and dinucleotides. However, considering the pentapeptide as a constant, it is still important in drug design to compare the relative interaction energies of different "chromophoric" isomers of actinomycin D. Even if the pentapeptide provides the driving force for association, one seeks the *least repulsive* chromophore–nucleotide interaction to maximize binding.

Summary and Conclusions

We have carried out simple electrostatic calculations on dinucleotides; we have evaluated the electrostatic potential for the ten dinucleotide base-pair combinations and evaluated the electrostatic interaction energies for substituted actinomycin chromophores with these dinucleotides. The results of the interaction energy calculations suggest that simple model calculations such as these might be useful in drug design of molecules that are "targeted" to interact with nucleotides.

Computational Details

We carried out STO-3G calculations[12] on the various fragments of DNA and used the Mulliken charges to evaluate the electrostatic potential near the dinucleotide phosphates. Because such charges are relatively insensitive to H bonding and conformational changes,[7] we used the same set of charges for different combinations. The dielectric constant was taken as 1 throughout. Because we carried out calculations on particular fragments and then joined the fragments, there were small edge effects, which we "smoothed out" so that the net charge of a dinucleoside phosphate was −1.0 (see Table I). For example, we had to remove ~0.04 e^- from the guanine N-9 to correct for the fact that we did the ab initio calculation on guanine with a hydrogen on N-9. Most of the electrostatic potential calculations included in addition a +1 charge to represent a sodium ion, bifurcating the PO_2^- group at R(NaO) = 2.4 Å.

By comparing the charges we report in Table I to the various ones noted by Bloomfield et al.,[13] we find the agreement qualitatively reasonable. Ours is the first ab initio calculation to consider both bases and backbone in a consistent way (i.e., to use the same basis set to describe the charge distribution).

In a previous study of protein electrostatic potentials,[7] we were able to carry out some 4-31G calculations[14] on the peptide fragments in order to check our STO-3G results. In general, there

Table V. Role of Amide Side Chains in Actinomycin Dinucleotide Interactions[c]

interaction	G-C / G-C	G-C / C-G	C-G / G-C	T-A / T-A	T-A / A-T	A-T / T-A	T-A / C-G	A-T / C-G	A-T / G-C	T-A / G-C
side chain[a]	−3.81	−3.12	−4.08	−1.43	−2.08	−0.86	−2.35	−1.80	−2.50	−3.04
chromophore[b]	0.51	−0.94	−0.33	−1.33	−0.43	−1.20	−1.54	−1.39	+0.08	−0.08

[a] Electrostatic interaction of two amide groups with dinucleotide. [b] Electrostatic interaction of phenoxazone chromophore with dinucleotide. [c] The sum of side chain and chromophore interactions is equal to the interactions in Table III (2-NH_2, 7-H).

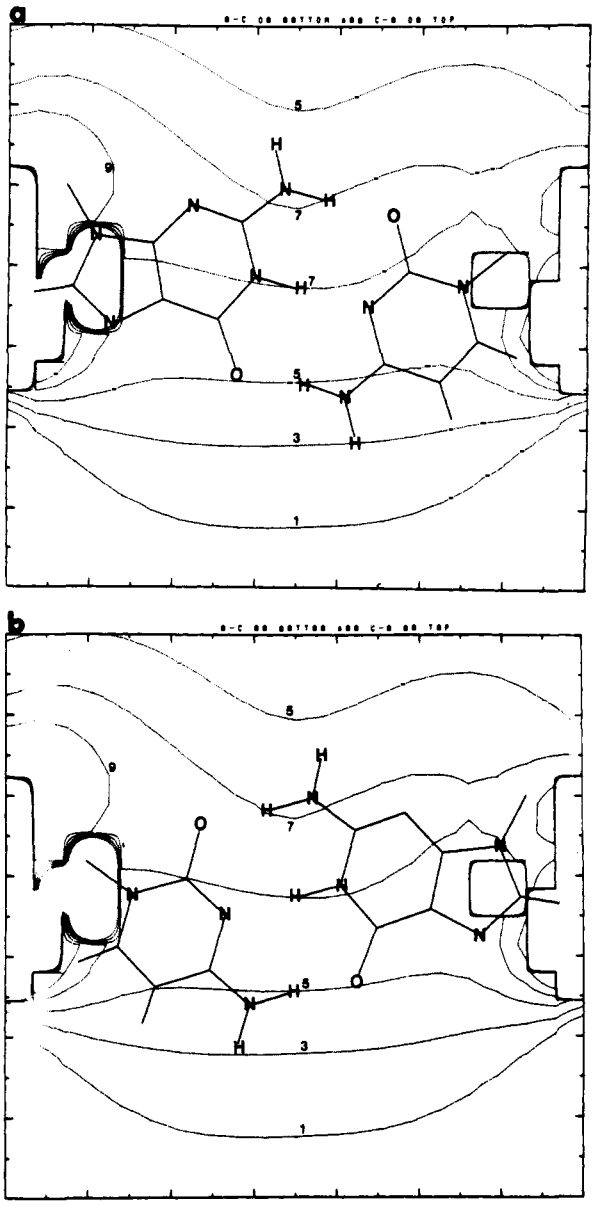

Figure 5. Projection of (a) C-G base pair onto electrostatic contour map and (b) G-C base pair onto electrostatic contour map.

was rather close agreement between the electrostatic potential results obtained with the two different basis sets, even though the Mulliken charges were very different for STO-3G vs. 431G. Unfortunately, the size of the systems and our computing budget precluded a similar comparison here.

Some of the substituted actinomycin intercalators here were too large for ab initio studies, so we used the CNDO/2[15] method to derive their Mulliken charges. For base–base interactions at ~3.4 Å, the results for the interaction energies and geometry calculated directly by CNDO/2 were in quite good agreement with those determined using the Mulliken charges derived from such calculations (see below).

We should stress at this point the difference between electrostatic potentials and electrostatic interaction energies. The electrostatic potential at a point represents the energy of a test

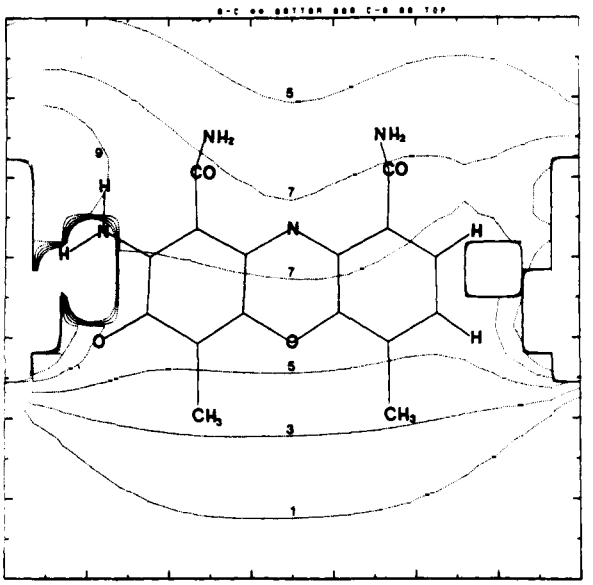

Figure 6. Projection of actinomycin D chromophore onto electrostatic contour map (see Figure 4). Because the actinomycin chromophore is not planar, not all its atoms lie in the plane. In particular, the 2-NH_2 does not lie in the excluded region.

charge (e.g., a proton without orbitals) placed at that point. The electrostatic potential gradient represents the energy of interaction of a *dipole* when placed in this gradient. We also present some calculations on model systems on the relevance of an electrostatic model, e.g., a comparison of the relative energies for cytosine–uracil rotation. The electrostatic energy alone (eq 1) is compared with

$$\Delta E_{ES} = \sum_{i,j} \frac{q_i q_j}{rij} \tag{1}$$

the electrostatic plus Lennard–Jones energies (eq 2) where the

$$\Delta E = \Delta E_{ES} + \sum_{i,j} \frac{A_{ij}}{r_{ij}^6} + \frac{B_{ij}}{r_{ij}^{12}} \tag{2}$$

A and B are from ref 16. We show that the electrostatic model is adequate, thus validating our use of it in Tables II–IV.

Note Added in Proof. Since this work has been completed (1977), these have been a series of very interesting papers by Pullman et al. on the electrostatic potential of nucleotides in a β DNA conformation, as well as the potentials due to base pairs. See, for example, ref 19.

Acknowledgment. We acknowledge the UCSF Academic Senate and the NIH (GM-20564) for research support, as well as the NIH (GM-70718) for a career development award to P.A.K.

References and Notes

(1) L. S. Lerman, *J. Mol. Biol.*, **3**, 18 (1961).
(2) H. M. Sobell and S. C. Jain, *J. Mol. Biol.*, **68**, 21 (1972).
(3) C. J. Alden and S. Arnott, *Nucleic Acid Res.*, **2**, 1701 (1975); *ibid.*, **4**, 3855 (1977).
(4) Reference 3 notes, however, that their model, unlike that of Sobell and Jain,[2] involves only dihedral angle changes and would thus be expected to be much less "strained".
(5) T. R. Krugh and J. W. Neely, *Biochemistry*, **12**, 4418 (1973).

(6) W. Muller and D. Crothers, *J. Mol. Biol.*, **35**, 251 (1968).
(7) D. M. Hayes and P. A. Kollman, *J. Am. Chem. Soc.*, **98**, 3335 (1976).
(8) H. Weinstein, D. Chou, S. Kang, C. L. Johnson, and J. P. Green, *Int. J. Quantum Chem.*, **QBS3**, 135 (1976).
(9) H. Weinstein, S. Masyani, S. Srebrenik, S. Cohen, and M. Sokolvosky, *Mol. Pharmacol.*, **9**, 820 (1973).
(10) G. Loew, D. S. Berkowitz, H. Weinstein, and S. Srebrenik in "Molecular and Quantum Pharmacology", B. Pullman and E. Bergmann, Ed., Dordrecht, Holland, 1975, p 355.
(11) P. Kollman, *J. Am. Chem. Soc.*, **99**, 4875 (1977).
(12) W. J. Hehre, R. F. Stewart, and J. A. Pople, *J. Chem. Phys.*, 51, 2651 (1969).
(13) V. Bloomfield, D. Crothers, and I. Tinoco, "Physical Chemistry of Nucleic Acids", Harper and Row, New York, 1974.
(14) R. Ditchfield, W. J. Hehre, and J. A. Pople, *J. Chem. Phys.*, **54**, 724 (1971).
(15) J. A. Pople, D. P. Santry, and G. A. Segal, *J. Chem. Phys.*, **43**(S), 129 (1965).
(16) F. A. Momamy, L. M. Carruthers, R. F. McGuire, and H. A. Scheraga, *J. Phys. Chem.*, **78**, 1595 (1974).
(17) J. Meisenhofer, *Cancer Chem. Rep.*, **58**, 21 (1974).
(18) F. Quadofoglio and V. Crescenzi, *Biophys. Chem.*, **2**, 64 (1974).
(19) D. Perahia, A. Kollman, and B. Pullman, *Theor. Chim. Acta*, **51**, 349 (1971).

Design of Species- or Isozyme-Specific Enzyme Inhibitors. 2.[1] Differences between a Bacterial and a Mammalian Thymidine Kinase in the Effect of Thymidine Substituents on Affinity for the Thymidine Site

Alexander Hampton,* Francis Kappler, and Ram R. Chawla

The Institute for Cancer Research, The Fox Chase Cancer Center, Philadelphia, Pennsylvania 19111.
Received March 19, 1979

Derivatives obtained by monosubstitution at six positions of thymidine, 5′-amino-5′-deoxythymidine, or 5-bromo-5,6-dihydrothymidine have been studied as inhibitors of *Escherichia coli* and hamster thymidine kinases (TK). Affinity for the enzymatic thymidine binding sites was assessed from apparent enzyme–inhibitor dissociation constants (K_i values; for inhibitions competitive with respect to thymidine at near-saturating ATP levels) or I_{50} values (for noncompetitive inhibitions). To provide indices of relative affinity for each enzyme, the K_i and I_{50} values were divided by the appropriate K_M value (33 or 3.3 μM) of thymidine with the *E. coli* and hamster enzymes, respectively. 3-Amylthymidine gave $I_{50}/K_M = 20$ with *E. coli* and $K_i/K_M = 21$ with hamster TK; 5-amino-2′-deoxyuridine gave $I_{50}/K_M = 840$ with *E. coli* TK and $K_i/K_M = 135$ with hamster TK; *trans*-5-bromo-6-ethoxy-5,6-dihydrothymidine diastereoisomers at 16 mM showed almost no inhibition of *E. coli* TK and gave $K_i = 0.2$–0.3 mM with hamster TK; 3′-acetamido- and 3′-(ethylthio)-3′-deoxythymidines gave $I_{50}/K_M = 183$ and 9.6, respectively, with *E. coli* TK and $K_i/K_M = 750$ and 3.6, respectively, with hamster TK; 5′-*C*-(acetamidomethyl)- and 5′-*C*-(propionamidomethyl)thymidine epimers inhibited both enzymes competitively ($K_i/K_M = 26$–198 for *E. coli* and 20–330 for hamster), and the extra methyl present in the propionamido derivatives produced 7.5- and 9-fold differential effects on binding; 5′-amino-5′-deoxythymidine also inhibited competitively ($K_i/K_M = 9.6$ for *E. coli* and 1.8 for hamster), and addition of a 5′-*N*-hexyl group reduced the differential affinity ($K_i/K_M = 78$ for *E. coli* and 54 for hamster); some 5′-(alkylthio)-5′-deoxythymidines inhibited hamster TK competitively but activated *E. coli* TK, possibly by interacting at its dCDP–dCTP activator site. The evidence indicates that thymidine derivatives suitably substituted at any one of the above six positions can bind to the thymidine sites of the *E. coli* and hamster thymidine kinases in a species-selective manner.

Increasing evidence indicates that enzymes from different species which catalyze an identical reaction are frequently structurally dissimilar from each other at regions that are situated outside the enzymatic active sites. In view of this, B. R. Baker[2] proposed that one approach to the design of species-selective enzyme inhibitors could be to determine a position of a substrate or a substrate analogue at which a substituent could be attached without preventing binding to the substrate site of the target enzyme and to vary the nature of the substituent with the object of bringing about differential reversible enzyme inhibition. This type of approach to species-specific inhibitors has been successfully utilized in studies with dihydrofolate reductases,[3-5] thymidine phosphorylases,[6] and adenylate kinases.[7] Baker[2] also suggested that the design of species-selective enzyme inhibitors might be aided by incorporation of a leaving group into the substituent, because species-specific neighboring group effects could come into play during displacement of such a group by a nucleophilic group of the target enzyme. This approach has subsequently given rise to several well-documented examples of substrate-site-directed reagents which bring about species-selective irreversible enzyme inhibition.[8-10]

Another potentially useful approach in the design of species-selective enzyme inhibitors would comprise attaching relatively small substituents to a substrate with the object of permitting or possibly promoting binding to the substrate site of the target enzyme while hindering or possibly preventing binding to the substrate site of the same enzyme from another species. The present report, which describes the first of several studies of this approach, is concerned with the interaction of *E. coli* and hamster thymidine kinases with a series of compounds obtained by monosubstitution at six positions of thymidine, 5′-amino-5′-deoxythymidine, or 5-bromo-5,6-dihydrothymidine. Positions of substitution were selected on the basis of synthetic accessibility but were representative of most areas of the thymidine molecule. For the most part, the substituents selected were short, relatively flexible, and nonbulky in order to increase the probability that they could permit binding to thymidine sites. The affinity of the compounds for the thymidine binding site of the *E. coli* enzyme has been evaluated by kinetic analysis of their inhibition of the enzyme-catalyzed reaction in the presence of near-saturating levels of the second substrate, ATP. The results have been compared with the previously reported

0022-2623/79/1822-1524$01.00/0